

A computational study of the malonic acid
tautomerization products in highly concentrated
particles.

Marilú Dick-Pérez and Theresa L. Windus

Department of Chemistry and Ames Laboratory, Iowa State University, Ames, Iowa 50011

ABSTRACT: Knowing the tautomeric form of malonic acid (MA) in concentrated particles is critical to understanding its effect on the atmosphere. Energies and vibrational modes of hydrated MA particles were calculated using density functional theory (DFT) at the B3LYP/6-31G(d,p) level and the effective fragment potential (EFP) method. Visualization of the keto and enol isomer vibrational modes enabled the assignment of keto isomer peaks in the 1710-1750 cm^{-1} range and previously unidentified experimental IR peaks in the 1690-1710 cm^{-1} can now be attributed to the enol isomer. Comparison of calculated spectra of pure hydrated enol or keto isomers confirm recent experimental evidence, presented by Ghorai et al,¹ of a shift in the keto-enol tautomer equilibrium when MA exists as concentrated particles.

INTRODUCTION

Small organic molecules found in the atmosphere are thought to affect global climate,^{1,2} cloud formation,³ and atmospheric reactions.⁴ One such compound is the three carbon dicarboxylic acid, malonic acid (MA, Figure 1). In solution, malonic acid undergoes keto-enol tautomerization with an equilibrium constant that is estimated to be less than 10^{-4} , favoring the keto form.⁵ However, a recent study provides evidence that the enol form is the major tautomer when MA exists as a concentrated particle in low humidity conditions:¹ the way MA is thought to behave in atmospheric pollutants.⁶ Higher concentrations of the enol (e-MA) versus the keto form (k-MA) of MA in particles indicate the need to further study the enol tautomer, which is absent in most MA studies.

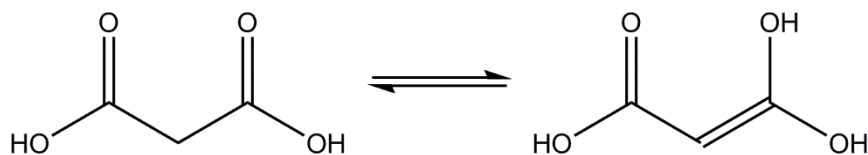


Figure 1. Malonic acid in the keto form (left) and enol form (right).

MA particles are hygroscopic, taking up water with increasing relative humidity (RH). The dry solid particles deliquesce at 73.7%, 79% and 86.6% RH at 293 K, 280.5 K and 243 K, respectively.⁷ The percent RH at which particles deliquesces suggests that spectroscopic results for a water to solute ratio (WSR) greater than 4 (~74% RH) should start resembling the solution phase results where MA is primarily in the keto form. Ghorai and co-workers observe infrared bands they assigned to e-MA from as low as ~2% RH (equilibrium constant for the tautomerization ~0.2) to as high as 90% RH (equilibrium constant ~2) in experiments conducted at 295 K.¹ Additionally, they observe a peak, thought to correspond to the enol, in concentrated MA solutions which suggests that a larger enol concentration is also found in concentrated MA

solutions than in dilute ones. However, equilibrium constants for the concentrated solutions were not reported¹ and could not be found in the literature.

As a solid dry MA particle, the majority of the MA molecules are in the keto-tautomer. As the particle deliquesces due to an increase in the RH, the system starts to resemble a liquid solution—a highly concentrated MA solution. The mechanism by which k-MA tautomerizes in concentrated solutions and highly concentrated deliquesced particles is not well understood. An intramolecular tautomerization requiring a high energy four membered ring transition state, as suggested by a gas phase study, is unlikely.⁸ A more likely mechanism is a 6-water mediated tautomerization transition state as previously proposed based on DFT calculations.⁸

The k-MA conformer has been the focus of various structural studies based on semiempirical, Hartree-Fock, and DFT calculations.⁹ The frequency values calculated for a single minimum energy structure of k-MA using HF with different basis sets (4-21G and 6-31G**) were shown to vary slightly from experimental IR and Raman frequencies.¹⁰ A more recent structural and vibrational study on various gas phase k-MA conformers using B3LYP and MP2 with 6-31G(d,p), 6-311G(2d,2p) and 6-311++(3df,3pd) basis sets show results consistent with experiment.¹¹

The e-MA isomer has been studied to a lesser degree. The deprotonated forms of both k- and e-MA were studied by Deerfield et al.¹² A structural and vibrational study of both k-MA and e-MA has not been found in the literature, thus prompting the current work.

To better understand e-MA's role in hydrated MA clusters, as prompted by the experimental evidence that e-MA is a significant component within concentrated MA particles, a computational study of MA cluster vibrational modes with varying hydration was undertaken. In this study, only clusters that include all e-MA or all k-MA with varying amounts of water are

examined. An overview of the cluster energetics is included for completeness. Though a more complete statistical mechanics treatment of the clusters may provide further insight into the energetics and hydrogen bonding trends, that treatment is outside the focus of this paper. Future studies on the tautomerization mechanism, a more complete study of the ensembles involved in the thermodynamics, and combinatorial effects of varying amounts of both structures in a given MA cluster, while outside of the scope of this study, are likely to provide further insight into the varying e-MA and k-MA concentrations observed.

METHODOLOGY

The MA cluster sizes were chosen based on the water to solute ratios (WSR) used by Ghorai and coworkers, where MA particles were exposed to conditions of varying relative humidity and correlated to their WSR.¹ The compositions of the simulated clusters were chosen to approximate the WSR in experimental conditions. The experimental RHs, approximate WSRs and simulated cluster sizes are reported in Table 1, where n_w and $n_{k/e}$ represent the number of water molecules and the number of k- or e-MA molecules, respectively. The simulated clusters contain either k- or e-MA only, thus focusing on determining the general differences between clusters made from each of the two tautomers.

Table 1. The number of molecules, water (n_w) or malonic acid (k- or e-MA, $n_{k/e}$) comprising clusters with the water to solute ratios and RH from experiment.¹

RH (%)	WSR (approximate)	Simulated Clusters ($n_w : n_{k/e}$)
90	10	10:1
83	6	6:1
74	4	4:1
62	1	1:1, 2:2
42	0.5	1:2
21	0.2	1:5
6	0	0:1, 0:2, 0:5

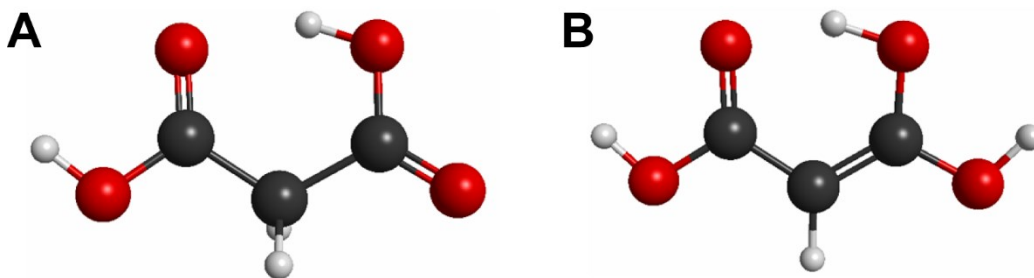


Figure 2. Minimum energy structures of A.) k-MA and B.) e-MA calculated using B3LYP/6-31G(d,p). Color scheme: oxygen, red; carbon, black; and hydrogen, white.

The level of theory used to calculate the final energies and vibrational frequencies for the k-MA (Figure 2A) and e-MA (Figure 2B) clusters was B3LYP/6-31G(d,p)^{13, 14} which has been shown to give the same energy ordering as MP2/6-311++G(3df,3pd) for k-MA conformers.¹¹ The size and number of structures to be studied limits the level of theory and basis. However, B3LYP has been previously used to study similar hydrated clusters with oxalate, a smaller dicarboxylic acid.¹⁵ All calculations were run using the GAMESS electronic structure code.¹⁶

To efficiently sample the many possible conformations of clusters containing more than a few molecules, the effective fragment potential (EFP) method and Monte Carlo based global optimizations with simulated annealing were used.¹⁷ In the EFP method, internally rigid molecular fragments are represented by model potentials that are fully derived from first principle, *ab initio* information. This allows cost effective modeling of large clusters by circumventing the explicit calculation of intramolecular interactions within fragments and by representing the intermolecular interactions with the model potential. Additional structures were determined by arranging the molecules by hand and maximizing hydrogen bonding.

The individual EFP molecules of enol, ketone and water were constructed using MP2/6-31++G(d,p).^{14, 18} The MA EFP molecules were created from both minimum energy structures and structures which were rotated about a CCCO dihedral angle in order to allow for more hydrogen bonding between the rigid fragments. Global optimizations with simulated annealing were used to find low energy structures starting from randomized fragment positions. For the simulated annealing calculations, the initial temperatures ranged from 5000 K to 3000 K and the final temperature of 100 K was set to be reached in five steps. Low energy structures were then fully optimized with B3LYP/6-31G(d,p) without any geometric constraints. While extensive simulations were run to try to obtain the lowest energy clusters, there is no guarantee that all of the lowest energy structures have been found. Positive definite Hessians at the B3LYP/6-31G(d,p) level confirmed the structures as minima on the potential energy surface, provided simulated IR frequency spectra and zero point energies (ZPE) for corrected energies. For comparisons with experiments, frequency values were scaled by 0.97, as suggested for a similar level of theory by Merrick and coworkers.¹⁹ MA vibrational mode assignments were determined by visualizing modes in MacMolPlt,²⁰ in some cases vibrations are delocalized such that traditional assignments (stretch/bend/wag) are difficult to determine.

The cluster binding energy (E_b) was taken to be the difference between the energy of the total cluster (E_c) and that of the isolated molecules, where E_w is the energy of water, and $E_{k/e}$ is the energy of k-MA or e-MA as appropriate. The E_b equation can be written as:

$$E_b = E_c - (n_w E_w + n_{k/e} E_{k/e})$$

The binding energies represent the stabilization due to intermolecular interactions since the isolated molecules include intramolecular interactions.

All energies reported include ZPE corrections. Relative energies between keto and enol structures were determined by subtracting the total energy of the e-MA clusters (monomer, dimer, and various WSR clusters) from the corresponding k-MA cluster.

RESULTS AND DISCUSSION

Vibrational Analysis

Experiments show that as the particle WSR increases, various FTIR peaks change in intensity.¹ By subtracting the 2% RH spectrum from higher RH spectra, the differences become clearer. The peaks that increase in intensity as the RH gets higher, from 2% to 90%, remain positive while the peaks that decrease in intensity as the RH increases, become negative. Based on previous assignments derived from similar systems and computational studies,^{11, 21} the assignments of negative peaks in the difference spectra are thought to correspond to vibrational modes of k-MA.¹ The positive peaks remain largely unassigned due to the lack of experimental and computational data available for cross-reference.

Calculated spectra of clusters containing 1 e/k-MA and 0, 1, 4, 6, and 10 water molecules in Figure 3 are plotted with positive intensities for e-MA clusters and negative for k-MA clusters. This data is explicitly for the lowest lying structures in each type of cluster. However, examining other structures within 1 kcal/mol of the lowest lying structure does not qualitatively change any of the results. Notable regions where experimental peaks are positive or negative are highlighted by purple and green boxes, respectively. Significant overlap exists between the e- and k-MA spectra, however, regions with peaks unique to e- or k-MA show good agreement with experimental observations. For example, from ~ 1730 - 1760 cm^{-1} where k-MA has many C=O stretch modes and e-MA does not, one can see several negative peaks but no positive ones.

More peaks associated with the coupled carbonyl-alkene stretching modes of e-MA, appear at lower wavenumbers, ~ 1615 - 1720 and ~ 1530 - 1585 cm^{-1} .

Other noteworthy peaks are the COH bending (~ 1435 - 1450 cm^{-1}); and methylene bending (~ 1410 cm^{-1}), wagging (~ 1210 - 1255 and ~ 900 - 950 cm^{-1}) and rocking (~ 925 - 955 cm^{-1}) modes unique to k-MA. Other modes unique to e-MA include: C=C stretch at ~ 1250 - 1320 cm^{-1} and a C=CH wag at ~ 1150 cm^{-1} . Experimental¹ and calculated values are reported in the Supporting Information (Table S1).

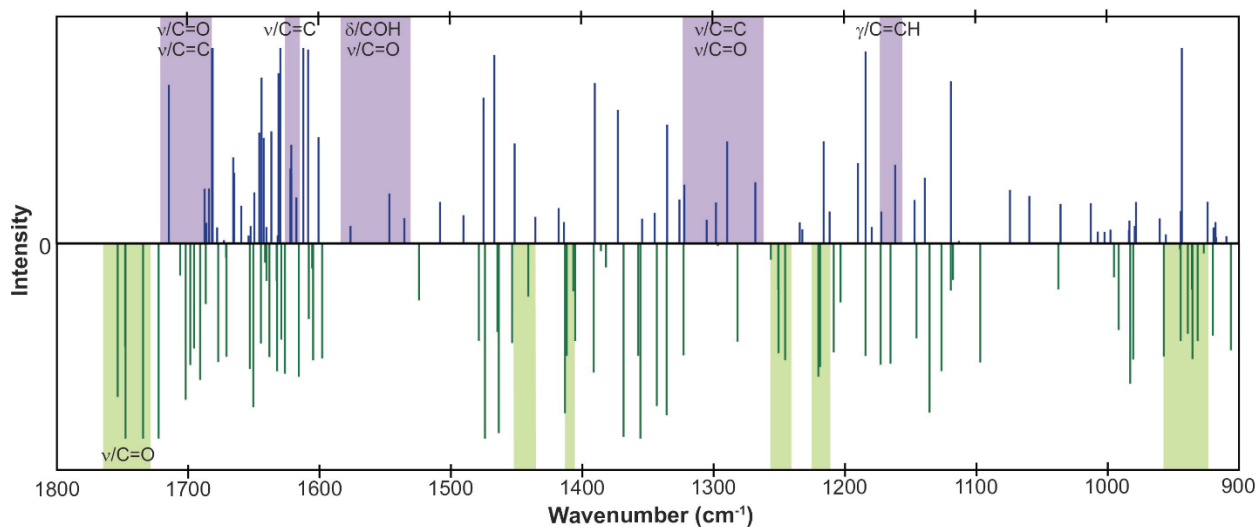


Figure 3. Malonic acid calculated vibrational modes for single MA molecules with WSR between 0 and 10. Enol (purple) and keto (green) vibrational frequencies plotted positive and negative, respectively. Shaded sections indicate positive (purple) and negative (green) peaks found in the difference spectra from Ghorai and co-workers.¹

Energetics

MA clusters containing various amounts of MA and water molecules were studied to better understand the relative keto to enol concentrations between dilute solutions and highly concentrated MA particles. Each cluster size, composition, number of different hydrogen bonds

and relative energy is found in Table 2. The composition of the cluster is designated by “MA” and “W” which refers to the number of MA molecules, either k-MA or e-MA, and water, respectively. Figures of the minimum energy structures and corresponding energies are provided in the Supporting Information.

The minimum energy clusters of k-MA are always lower in energy than the e-MA clusters (positive energy differences, ΔE , in Table 2). The degree to which the k-MA clusters are more stable than the e-MA clusters is likely an artifact of studying small structures. For example, for a 0% RH (zero waters in the cluster), the relative energy varies greatly, from about 6 kcal/mol (0:1 for W:MA ratio) to 65 kcal/mol (0:5 for W:MA ratio). It is also possible that the lowest energy minimum for a given cluster was not found even after extensive structure searches. Therefore, direct comparison of the relative energies within and between the different WSR clusters is hampered. However, all the clusters with 1 MA exhibit a general trend of increasing energy gap with increasing number of waters. In the 2-MA clusters, the trend is even more pronounced. These observations are consistent with the experimental observation that the enol is more prevalent at lower RH and WSR.

In general, the k-MA cluster's much lower energy may be explained by its ability to rotate about the CCCO dihedral angle, allowing it to form additional hydrogen bonds. For example, Figure 4A shows the lowest energy (k-MA)₅ cluster where intermolecular hydrogen bonding is maximized by rotating about the CCCO dihedral angle. The (e-MA)₅ (Figure 4B) does not break planarity due to the C-C double bond and thus cannot maximize the hydrogen bonded network. While not likely to be found in nature due to entropic effects, this five k-MA ring's hydrogen bonding network affords 65.3 kcal/mol stabilization over (e-MA)₅ (Table 2).

Table 2. The number and types of hydrogen bonds (H-bonds) for each cluster composition, number of water and MA molecules per cluster, are given with respect to WSR. The types of hydrogen bonds (H-bonds) include: intramolecular k-MA, and e-MA; intermolecular between malonic acid and water (MA-w), between water molecules (w-w), and between malonic acid molecules (MA-MA). The total number of hydrogen bonds (Total H-bonds) are given for k-MA and e-MA. Finally, the k-MA and e-MA binding energies, E_b , and the energy difference between k-MA and e-MA minimum energy structures, ΔE , are given in kcal/mol.

		WSR	Intra-molecular		Intermolecular						Total		E_b		ΔE
W	MA		K	E	MA-w		w-w		MA-MA		H-bonds		(kcal/mol)		
					K	E	K	E	K	E	K	E	K	E	
0	1	0	1	1	-	-	-	-	-	-	1	1	0.0	0.0	5.5
0	2	0	2	2	-	-	-	-	2	2	4	4	-15.7	-17.3	9.5
0	5	0	0	5	-	-	-	-	10	6	10	11	-86.7	-50.1	64.3
1	5	0.2	0	5	0	2	-	-	10	5	10	12	-92.2	-58.2	61.7
1	2	0.5	0	2	2	4	-	-	1	0	3	6	-19.6	-18.5	12.1
1	1	1	1	1	2	2	-	-	-	-	3	3	-9.8	-4.7	10.6
2	2	1	1	2	4	3	0	0	1	2	6	7	-41.0	-38.6	13.5
4	1	4	0	1	4	2	3	3	-	-	7	6	-49.6	-39.7	15.5
6	1	6	1	1	3	5	6	6	-	-	10	12	-73.8	-68.7	10.6
10	1	10	0	0	5	6	12	12	-	-	17	18	-124.1	-114.0	15.6
20	2	10	0	0	12	16	26	25	0	0	38	41	-277.0	-245.0	43.1

W, water; MA, malonic acid; K, keto-MA; E, enol-MA; MA, malonic acid.

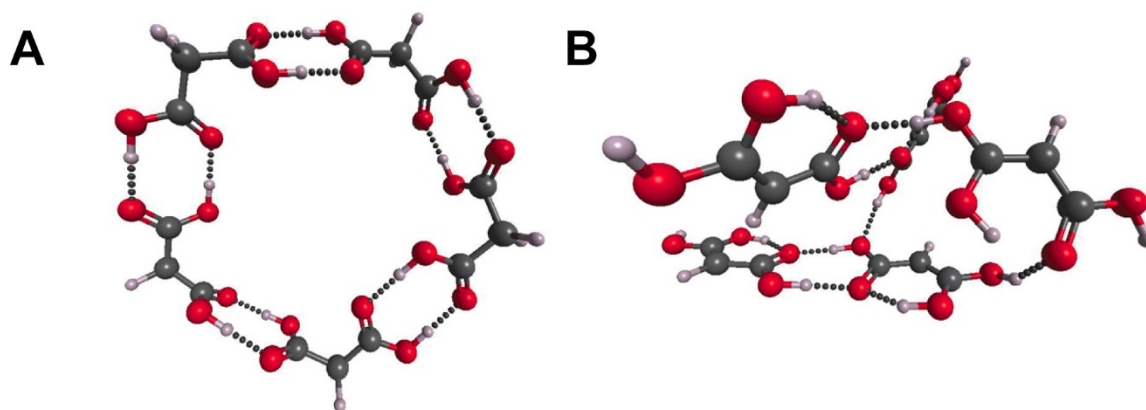


Figure 4. Clusters of five A.) k-MA and B.) e-MA. The keto form can rotate about the CCCO to accommodate efficient intermolecular hydrogen bonding while the enol form cannot.

As another example, the lowest energy structures for k-MA and e-MA with 10 waters is shown in Figure 5A. The four-water motifs formed by waters-(1, 2, 3, 4) and (6, 7, 8, 9) are similar to the stable four-water motifs found in low-energy water clusters comprised of 4, 5, or 6 waters.²² The enol structure also exhibits similar water conformations, however, the four-water (1, 2, 3, 4), motif is distorted and is not stabilized by e-MA as it is in the k-MA cluster. The difference in hydrogen bond lengths, 1.72 Å in the k-MA structure (Figure 5A, highlighted in green) versus 2.54 Å in the e-MA structure (Figure 5B), also indicates that the H-bond is stronger in k-MA structure. Where the carbonyl group in k-MA can bend towards the waters (highlighted in green, Figure 5A), e-MA is restricted by the planar C-C-C geometry. At a 10:1 water to solute ratio, the enol structure is no longer internally hydrogen bonded, likely from the hydroxyl group being stabilized by hydrogen bonding to water.

Interestingly, even in clusters containing more waters, the MA tends to be on the outside of the water cluster. The water dimer binding energy is the same as the 1:1 e-MA binding energy (-4.7 kcal/mol), while the 1:1 k-MA binding energy is -9.8 kcal/mol (Table 2). However, the k-MA

and e-MA dimer binding energies (0:2 ratio in Table 2) is -15.7 and -17.3 kcal/mol, respectively. The preferential MA-MA binding suggests that clusters containing multiple MA and water molecules would likely form separate MA and water regions. Also, waters can make more hydrogen bonds in larger clusters allowing the creation of a water network that mostly excludes the MA. The total number of hydrogen bonds in the other low energy structures follows the same trend (Table S3) as the minimum energy structures in Table 2. A scan of the other low energy clusters show some deviations with some water molecules preferentially binding to MA rather than forming part of the water network (specifically in Figure S3B and S4).

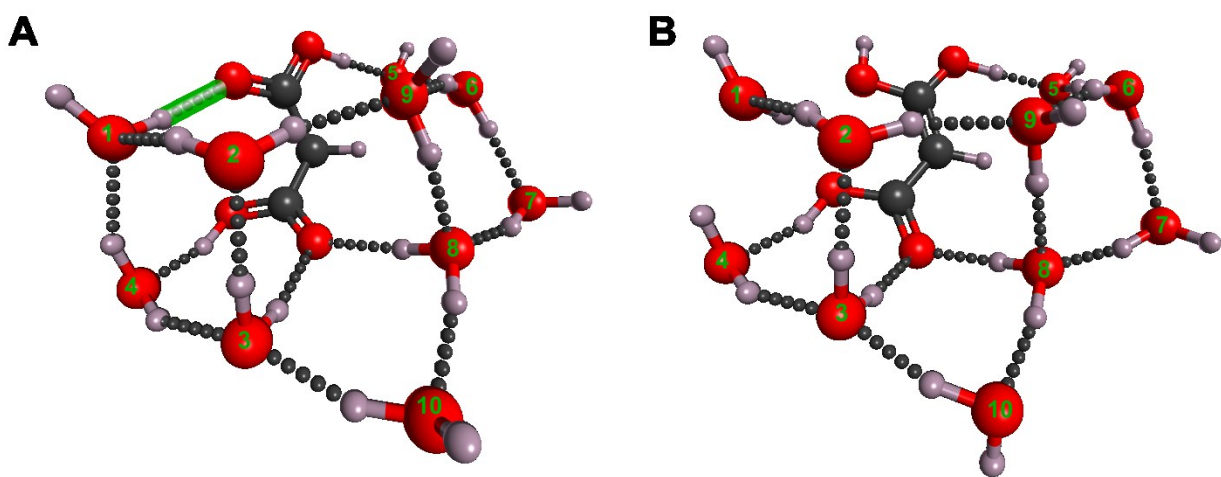


Figure 5. One malonic acid, (A) k-MA and (B) e-MA, surrounded by 10 water molecules. The keto structure rotates about the CCCO dihedral angle to accommodate more hydrogen bonds (MA to water number 1, highlighted in green). The water molecules are labeled for reference, see text.

Hydrogen Bonding Network

Unsurprisingly, the total cluster energy appears to be correlated to inter- and intramolecular hydrogen bonds. The number and types of hydrogen bonds (inter-, intramolecular, water-water,

water-MA) can be found in Table 2. The e-MA forms an intramolecular hydrogen bond in all clusters except for the highest WSR, 10:1. There is no direct correlation between number/type of hydrogen bonds and the relative stability between k/e-MA structures (energy difference in Table 2) but the binding energy has a linear relationship to the total number of hydrogen bonds, Figure 6. The e-MA clusters show slightly greater linearity with an R^2 value of 0.991 than k-MA clusters with an R^2 value of 0.986. This linear relationship indicates that hydrogen bonds are the main stabilizing interaction in clusters.

The greater slope in the k-MA systems may indicate why it is more stable than the e-MA systems in solution, though further testing would be necessary to confirm this. Of the lower concentrations studied experimentally, 1 M and 4 M MA solutions corresponding to 55.5 and 12.9 WSRs, respectively, 4 M was the lowest concentration where e-MA is the more abundant tautomer.¹ At low concentrations of MA, water likely lowers the tautomerization reaction barrier producing the experimentally observed and thermodynamically stable k-MA.⁸

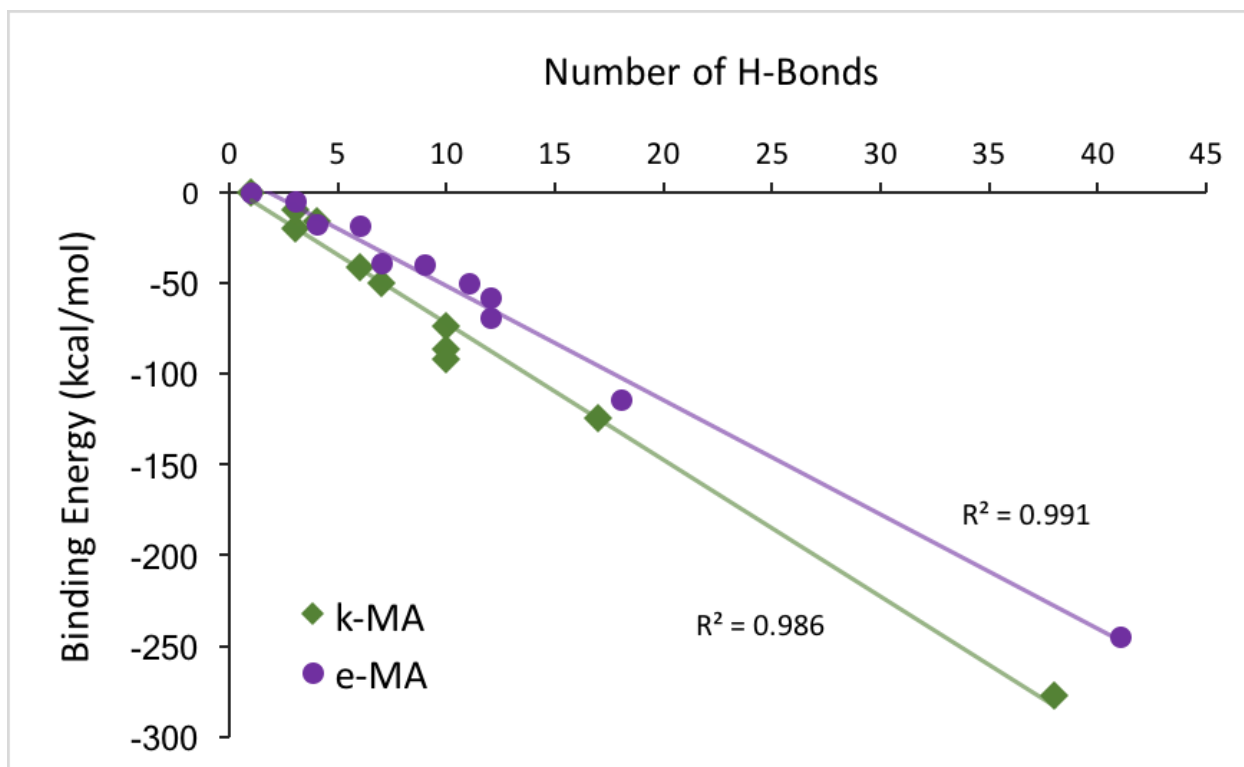


Figure 6. Relationship between number of hydrogen bonds and binding energy for e-MA (circles, $R^2=0.991$) and k-MA (diamond, $R^2=0.986$).

CONCLUSION

MA clusters containing various water to solute ratios were reported experimentally to have high enol concentrations. Based on the calculations of MA in water, the vibrational modes match the observed increases and decreases in FTIR spectra confirming the appearance of the e-MA.

It should be noted that cluster calculations containing a mixture of k-MA and e-MA would be needed to fully explore the stability of the cluster. However, the current results do suggest that larger cluster effects shift the keto-enol tautomerization equilibrium towards e-MA in concentrated MA particles.

As expected, hydrogen bonding is the major contributor to cluster binding energies. The MA-water hydrogen bonds help explain the cluster stability with the flexibility of the k-MA providing

additional possibilities for more stable structures. At low MA concentrations, the stability of the system depends less on water interacting with MA and more on water-water interactions. The energetic stability dependence on interaction types is consistent with the observed increase in e-MA hydroxyl-group rotation flexibility when more water molecules are present.

The results from our study mainly focus on the comparison of simulated results to the solid concentrated MA particles but could potentially be applied to solution studies as well. Most importantly, the assignment of the e-MA IR frequencies further confirms that the e-MA isomer composes the major form of MA in concentrated MA particles and should not be ignored in future MA studies.

Supporting information. Molecular structure images, minimum energy structure coordinates, vibrational mode absorption frequency assignments supplied as Supporting Information.

ACKNOWLEDGEMENT

The authors would like to thank the reviewers and the Windus Group members for invaluable discussion and help with manuscript preparation. This research is sponsored in part (MDP) by the Graduate Minority Assistantship Program (GMAP), a program in the Graduate College at Iowa State University that provides support to underrepresented students pursuing masters and PhD degrees. This research is sponsored in part (TLW) by the U.S. Department of Energy, Office of Basic Energy Sciences, Division of Chemical Sciences, Geosciences, and Biosciences through the Ames Laboratory Chemical Physics project. Ames Laboratory is managed by Iowa State University for the USDOE under contract DE-AC02-07CH11358.

ABBREVIATIONS

DFT, density functional theory; EFP, effective fragment potential; e-MA, enol-malonic acid; FTIR, Fourier transform infrared spectroscopy; HF, Hartree-Fock; IR, infrared spectroscopy; k-MA, keto-malonic acid; RH, relative humidity; WSR, water to solute ratio; ZPE, zero-point energy.

REFERENCES

1. Ghorai, S.; Laskin, A.; Tivanski, A. V. Spectroscopic evidence of keto-enol tautomerism in deliquesced malonic acid particles. *The journal of physical chemistry. A* **2011**, *115* (17), 4373-80.
2. Karcher, B.; Koop, T. The role of organic aerosols in homogeneous ice formation. *Atmospheric Chemistry and Physics* **2005**, *5* (3), 703-714; Posfai, M.; Buseck, P. R. Nature and Climate Effects of Individual Tropospheric Aerosol Particles. *Annual Review of Earth and Planetary Sciences* **2010**, *38* (1), 17-43.
3. Sun, J.; Ariya, P. A. Atmospheric organic and bio-aerosols as cloud condensation nuclei (CCN): A review. *Atmospheric Environment* **2006**, *40* (5), 795-820; Prenni, A. J.; DeMott, P. J.; Kreidenweis, S. M.; Sherman, D. E.; Russell, L. M.; Ming, Y. The Effects of Low Molecular Weight Dicarboxylic Acids on Cloud Formation. *Journal of Physical Chemistry A* **2001**, *105*, 11240-11248.
4. Kroll, J. H.; Seinfeld, J. H. Chemistry of secondary organic aerosol: Formation and evolution of low-volatility organics in the atmosphere. *Atmospheric Environment* **2008**, *42* (16), 3593-3624.
5. Leopold, K. R.; Haim, A. Equilibrium, kinetics, and mechanism of the malonic acid-iodine reaction. *International Journal of Chemical Kinetics* **1977**, *9* (1), 83-95.
6. Chebbi, A.; Carlier, P. Carboxylic acids in the troposphere, occurrence, sources, and sinks: A review. *Atmospheric Environment* **1996**, *30* (24), 4233-4249; Kawamura, K.; Sakaguchi, F. Molecular distributions of water soluble dicarboxylic acids in marine aerosols over the Pacific Ocean including tropics. *Journal of Geophysical Research* **1999**, *104* (D3), 3501-3509; Kawamura, K.; Kasukabe, H.; Barrie, L. A. Source and reaction pathways of dicarboxylic acids, ketoacids and dicarbonyls in arctic aerosols: One year of observations. *Atmospheric Environment* **1996**, *30* (10-11), 1709-1722.
7. Parsons, M. T.; Mak, J.; Lipetz, S. R.; Bertram, A. K. Deliquescence of malonic, succinic, glutaric, and adipic acid particles. *Journal of Geophysical Research* **2004**, *109*, D06212; Pope, F. D.; Dennis-Smith, B. J.; Griffiths, P. T.; Clegg, S. L.; Cox, R. A.; Tong, H.-J.; Reid, J. P. Studies of Single Aerosol Particles Containing Malonic Acid, Glutaric Acid, and Their Mixtures with Sodium Chloride I Hygroscopic Growth. *The Journal of Physical Chemistry A* **2010**, *114* (37), 10156-10165.
8. Yamabe, S.; Tsuchida, N.; Miyajima, K. Reaction Paths of Keto-Enol Tautomerization of beta-Diketones. *Journal of Physical Chemistry A* **2004**, *108* (14), 2750-2757.
9. Merchán, M.; Tomás, F.; Nebot-Gil, I. An *ab initio* study of intramolecular hydrogen bonding in malonic acid and its monoanion. *Journal of Molecular Structure: THEOCHEM* **1984**, *109*, 51-60; Ajo, D.; Fragala, I.; Granozzi, G.; Tondello, E. Conformational analysis of malonic acid and its derivatives: *ab initio*, CNDO/2 and empirical calculations. *Journal of Molecular Structure* **1977**, *38*, 245-252; Nguyen, T. H.; Hibbs, D. E.; Howard, S. T. Conformations, energies, and intramolecular hydrogen bonds in dicarboxylic acids: implications for the design of synthetic dicarboxylic acid receptors. *Journal of computational chemistry* **2005**, *26* (12), 1233-41.
10. Tarakeshwar, P.; Manogaran, S. Conformations and vibrations of dicarboxylic acids An *ab initio* study. *Journal of Molecular Structure, Theochem* **1996**, *362*, 77-99.

11. Maçôas, E. M. S.; Fausto, R.; Lundell, J.; Pettersson, M.; Khriachtchev, L.; Räsänen, M. Conformational Analysis and Near-Infrared-Induced Rotamerization of Malonic Acid in an Argon Matrix. *Journal of Physical Chemistry A* **2000**, *104*, 11725-11732.
12. Deerfield II, D. W.; Pedersen, L. G. Enol and deprotonated forms of acetic and malonic acid. *Journal of Molecular Structure: THEOCHEM* **1996**, *368*, 163-171.
13. Becke, A. D. Density-functional thermochemistry III. The role of exact exchange. *The Journal of Chemical Physics* **1993**, *98* (7), 5648; Lee, C.; Yang, W.; Parr, R. G. Development of the Colle-Salvetti correlation-energy formula into a functional of the electron density. *Physical Review B* **1988**, *37* (2), 785-789.
14. Hariharan, P. C.; Pople, J. A. The Influence of Polarization Functions on Molecular Orbital Hydrogenation Energies. *Theoretica Chimica Acta* **1973**, *28*, 213; Hehre, W. J.; Ditchfield, R.; Pople, J. A. Self-Consistent Molecular Orbital Methods. XII. Further Extensions of Gaussian-Type Basis Sets for Use in Molecular Orbital Studies of Organic Molecules. *Journal of Chemical Physics* **1972**, *56*, 2257-2261; Ditchfield, R.; Hehre, W. J.; Pople, J. A. Self-Consistent molecular orbital methods. IX. An extended Gaussian-type basis for molecular orbital studies of organic molecules. *Journal of Chemical Physics* **1971**, *54*, 724-728.
15. Weber, K. H.; Morales, F. J.; Tao, F.-M. Theoretical Study on the Structure and Stabilities of Molecular Clusters of Oxalic Acid with Water. *Journal of Physical Chemistry A* **2012**, *116*, 11601-11617.
16. Schmidt, M. W.; Baldridge, K. K.; Boatz, J. A.; Elbert, S. T.; Gordon, M. S.; Jensen, J. H.; Koseki, S.; Matsunaga, N.; Nguyen, K. A.; Su, S.; Windus, T. L.; Dupuis, M.; Montgomery, J. A. General atomic and molecular electronic structure system. *Journal of Computational Chemistry* **1993**, *14* (11), 1347-1363; Gordon, M. S.; Schmidt, M. W. Advances in electronic structure theory: GAMESS a decade later. In *Theory and Applications of Computational Chemistry: the first forty years*, Dykstra, C. E.; Frenking, G.; Kim, K. S.; Scuseria, G. E., Eds. Elsevier: Amsterdam, 2005; pp 1167-1189.
17. Jensen, J. H.; Day, P. N.; Gordon, M. S.; Basch, H.; Cohen, D.; Garmer, D. R.; Kraus, M.; Stevens, W. J. Effective Fragment Method for Modeling Intermolecular Hydrogen-Bonding Effects on Quantum Mechanical Calculations. In *Modeling the Hydrogen Bond*, Smith, D. A., Ed. ACS Symposium Series: 1994; Vol. 569, pp 139-151; Gordon, M. S.; Slipchenko, L. V. L.; Li, H.; Jensen, J. H. The Effective Fragment Potential: A General Method for Predicting Intermolecular Interactions **2007**, *3* (07), 177-193; Metropolis, N.; Rosenbluth, A. W.; Rosenbluth, M. N.; Teller, A. H. Equation of state calculations by fast computing machines. *The Journal of chemical physics* **1953**, *21* (6), 1087-1092; Li, Z.; Scheraga, H. A. Monte Carlo-minimization approach to the multiple-minima problem in protein folding. *Proceedings of the National Academy of Sciences* **1987**, *84* (19), 6611-6615; Kirkpatrick, S.; Gelatt, C. D.; Vecchi, M. P. Optimization by simulated annealing. *Science (New York, N.Y.)* **1983**, *220* (4598), 671-80.
18. Moller, C.; Plesset, M. S. Note on an Approximation Treatment for Many-Electron Systems. *Physical Review* **1934**, *46* (7), 618-622; Aikens, C. M.; Webb, S. P.; Bell, R. L.; Fletcher, G. D.; Schmidt, M. W.; Gordon, M. S. A derivation of the frozen-orbital unrestricted open-shell and restricted closed-shell second-order perturbation theory analytic gradient expressions. *Theoretical Chemistry Accounts: Theory, Computation, and Modeling (Theoretica Chimica Acta)* **2003**, *110* (4), 233-253; Fletcher, G. D.; Schmidt, M. W.; Gordon, M. S. Developments in parallel electronic structure theory. In *Advances in Chemical Physics, Volume 110*, Prigogine, I.; Rice, S. A., Eds. John Wiley & Sons, Inc.: New York, NY, 1999; pp 267-294; Clark, T.; Ch; rasekhar, J.; Spitznagel, G. n. W.; Schleyer, P. V. R. Efficient diffuse function-

augmented basis sets for anion calculations III The 3-21+G basis set for first-row elements, Li-F. *Journal of Computational Chemistry* **1983**, *4* (3), 294-301.

19. Merrick, J. P.; Moran, D.; Radom, L. An evaluation of harmonic vibrational frequency scale factors. *The journal of physical chemistry. A* **2007**, *111* (45), 11683-700.

20. Bode, B. M.; Gordon, M. S. Macmolplt: a graphical user interface for GAMESS. *Journal of Molecular Graphics and Modelling* **1998**, *16* (3), 133-138.

21. Ganguly, S.; Fernandes, J. R.; Desiraju, G. R.; Rao, C. N. R. Phase transition in malonic acid: an infrared study. *Chemical Physics Letters* **1980**, *69* (2), 227-229; Cabaniss, S. E.; Leenheer, J. A.; McVey, I. F. Aqueous infrared carboxylate absorbances: aliphatic di-acids. *Spectrochimica Acta Part A: Molecular and Biomolecular Spectroscopy* **1998**, *54* (3), 449-458.

22. Xantheas, S. S. Cooperativity and hydrogen bonding network in water clusters. *Chemical Physics* **2000**, *258* (2-3), 225-231.

Table of Contents Graphic

